Pharmaceutical Sciences and Drug Design
ISSN: 3062-4428
2023, Volume 3, Page No: 224-238

Available online at: www.galaxypub.co/page/journals

Galaxy Publication

Galaxy Publication

A Network-Based Pharmacologic Analysis Combined With Experimental Confirmation Was Used to Unravel How Compound Huangbai Liquid Exerts Its Therapeutic Actions against Acne

Samantha King[1]*, Riley Adams[1]

[1]Department of Biotechnology, Faculty of Pharmacy, University of Oslo, Oslo, Norway.

***E-mail** ✉ samantha.king.no@gmail.com

Received: 24 May 2023; **Revised:** 27 August 2023; **Accepted:** 01 September 2023

ABSTRACT

Acne is a common dermatological condition in which inflammation plays a central role. Compound Huangbai Liquid (CHL), a well-known traditional Chinese medicine (TCM) formulation, has demonstrated notable clinical benefits for acne, yet its mechanistic basis has not been comprehensively clarified using an integrated network pharmacology strategy.We identified the bioactive constituents of CHL and their putative molecular targets using the BATMAN-TCM platform. Acne-associated genes were collected from GeneCards, DisGeNet, and OMIM. Potential therapeutic targets were screened through Venn analysis. Protein–protein interaction (PPI) mapping was conducted using the STRING database, and Cytoscape 3.9.1 was applied to construct the interaction network and extract core proteins. GO enrichment and KEGG pathway analyses were carried out using Metascape and bioinformatics.com.cn. Visualization of TCM-compound-target-disease associations and disease-target-pathway relationships was generated in Cytoscape. Lastly, a mouse acne model was used to experimentally validate the predicted mechanisms.A total of 165 active molecules, 1117 drug-related targets, 156 acne-associated genes, and 34 intersecting therapeutic targets were identified. Enriched biological functions mainly involved lipid-responsive processes, lipopolysaccharide-related signaling, and secretory regulation. CHL showed strong relevance to ten major pathways, including those associated with Chagas disease and cancer-related signaling. Animal testing confirmed that CHL markedly reduced inflammatory mediator levels and suppressed the TLR4/NF-κB/p38 MAPK pathway in the acne model.This work highlights the multi-compound, multi-target, and multi-pathway characteristics of CHL in combating acne, offering an expanded framework for understanding how traditional Chinese medicine exerts therapeutic effects in acne management.

Keywords: Inflammation, Compound Huangbai Liquid, Network pharmacology, Acne

How to Cite This Article: King S, Adams R. A Network-Based Pharmacologic Analysis Combined With Experimental Confirmation Was Used to Unravel How Compound Huangbai Liquid Exerts Its Therapeutic Actions against Acne. Pharm Sci Drug Des. 2023;3:224-38. https://doi.org/10.51847/XGJF2Ny0WO

Introduction

Acne is one of the most widespread chronic inflammatory conditions of the Skin [1], affecting over 85% of adolescents and often extending into adulthood, where it leaves issues such as hyperpigmentation and long-term scarring [2, 3]. Numerous factors contribute to its development—including hormonal fluctuations, microbial activity, and variations in sebum output—with abnormal sebum secretion regarded as a major driving element in Acne pathogenesis [4]. Although its origins are multifactorial, inflammation remains a defining biological hallmark [1, 5]. Extensive research now confirms that inflammatory signaling governs the initiation, progression, and even resolution of Acne lesions. Among the early inflammatory regulators, the IL-1 cytokine family acts as a pivotal initiating factor [6]. For example, Cutibacterium acnes markedly heightens IL-1β secretion in sebocytes [7], and increased IL-1 activity stimulates endothelial and vascular responses surrounding pilosebaceous units, setting off a broader inflammatory cascade [8]. IL-1β also enhances the production of IL-6 and IL-8 in sebocytes, underscoring its importance in Acne-associated inflammation [9]. Keratinocytes further contribute to disease

development, as P. acnes robustly induces IL-1β release from these cells in a dose-dependent fashion [10]. Beyond IL-1, inflammatory mediators such as IL-6, TNF, and IL-10 also participate in Acne-related immune responses [11]. Furthermore, Cutibacterium acnes activates toll-like receptors TLR-2 and TLR-4, which subsequently trigger MAPK and NF-κB signaling pathways [12]. Conventional treatments for Acne include retinoids, benzoyl peroxide, antibiotics, and hormonal agents [13], yet growing interest has turned toward Traditional Chinese Medicine (TCM) for its therapeutic benefits.

With thousands of years of clinical use [14], TCM has accumulated rich experience in dealing with dermatological disorders such as psoriasis, vitiligo, eczema, and Acne [15–18]. TCM therapies are generally accessible, cost-efficient, and associated with fewer adverse reactions, making them appealing in Acne care [15, 19]. Several classical prescriptions—including Qing-Shang-Fang-Feng-Tang, Zhen-Ren-Huo-Ming-Yin, Jia-Wei-Xiao-Yao-San, Wu-Wei-Xiao-Du-Yin, and Huang-Lian-Jie-Du-Tang—have been employed effectively for Acne management [15]. Among them, Compound Huangbai Liquid (CHL), comprising Forsythiae Fructus (Lianqiao), Phellodendri chinensis Cortex (Huangbai), Honeysuckle (Jinyin Hua), Dandelion (Pugong Ying), and Centipede (Wugong), has demonstrated remarkable therapeutic efficacy in China; however, its mechanistic basis remains insufficiently understood.

Network pharmacology offers a modern systems-level framework for unraveling how drugs, targets, and diseases interact within biological networks [20]. This methodology enables prediction and systematic interpretation of drug mechanisms [21]. In the present study, we identified the active pharmacological constituents of CHL, mapped their potential targets, and integrated these with Acne-related genes to obtain therapeutic intersection targets. Functional and pathway enrichment analyses were then applied to highlight key signaling mechanisms involved in CHL's activity, followed by experimental validation to support the computational predictions. The overall study design is presented in **Figure 1.**

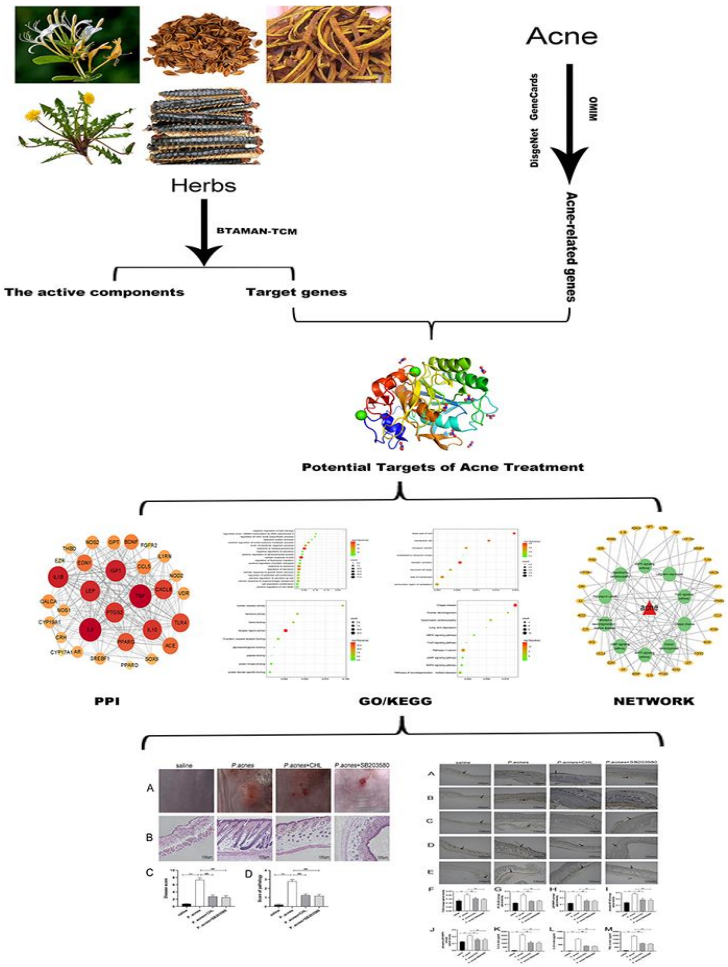

Figure 1. Schematic overview illustrating the analytical pipeline applied to investigate the actions of Compound Huangbai Liquid in acne management.

Materials and Methods

Drug and disease targets identification

To acquire the chemical constituents attributed to each herb in the formula, the BATMAN-TCM platform (http://bionet.ncpsb.org.cn/batman-tcm/) was queried using the terms "LIAN QIAO", "HUANG BAI", "JIN YIN HUA", "PU GONG YING", and "WU GONG". Compounds and their predicted molecular targets were retained only when their scoring index met or exceeded 20 and the statistical significance reached $P < 0.05$.

In parallel, genes associated with acne pathology were assembled by searching GeneCards (https://www.genecards.org), DisGeNet (https://www.disgenet.org/), and OMIM (https://omim.org/) using "acne" as the identifier.

Prediction of Compound Huangbai Liquid targets for acne treatment

Overlap between CHL-associated targets and acne-related genes was generated through the Venn mapping tool (http://bioinformatics.psb.ugent.be/webtools/Venn/). These intersecting genes were regarded as the likely therapeutic targets of CHL.

Construction and analysis of Protein–Protein Interaction (PPI) network

The predicted shared targets were imported into the STRING 11.0 database (https://string-db.org) to construct a protein interaction landscape. The resulting network was visualized using Cytoscape 3.9.1, enabling identification of proteins occupying central or highly connected positions within the PPI architecture.

Gene function and pathway enrichment analysis

Functional enrichment was performed to categorize target genes within Gene Ontology domains—biological processes (BP), cellular components (CC), and molecular functions (MF). Kyoto Encyclopedia of Genes and Genomes (KEGG) enrichment analysis (http://www.genome.jp/kegg/) was conducted to pinpoint signaling pathways implicated in CHL's activity. GO and KEGG analyses were executed via Metascape and bioinformatics.com.cn, applying $P < 0.05$ as the significance threshold for KEGG enrichment.

Network construction

To visualize how herbal ingredients, chemical components, predicted targets, biological pathways, and disease characteristics interrelate, Cytoscape 3.9.1 was used to construct two comprehensive network diagrams: the TCM-compound–target–disease network and the disease–target–pathway network.

Culture of Propionibacterium acnes (P. acnes) strains

Propionibacterium acnes (ATCC6919) purchased from BeNa Culture Collection was first propagated on blood agar and then transferred to BHI medium under anaerobic conditions at 37°C. The culture was diluted 1:100 in fresh BHI and expanded until the optical density at 600 nm reached 0.1–0.3. Cells were collected by centrifugation at 3220 g for 5 minutes, rinsed three times with BHI, and adjusted to approximately 1×10^7 CFU.

Preparation of synthetic sebum

Synthetic sebum was formulated from squalene, triolein, oleic acid, jojoba oil, and Vitamin E (±α-tocopherol), all obtained from Macklin (St Huatuo, Shanghai, China). Squalene had a purity of 98%, triolein and oleic acid 99%, jojoba oil 90%, and Vitamin E 95%. Each lipid component was dissolved in dichloromethane:methanol (2:1), and the final mixture used in experiments contained 17% oleic acid, 44.7% triolein, 25% jojoba oil, 12.4% squalene, and 0.9% Vitamin E.

Ethics statement and animal experiments

Male BALB/c mice free of specific pathogens (5–6 weeks old; 20–22 g) were supplied by the Peng Yue Experimental Animal Center (Jinan, China; permit SCXK 2022-0009). Ethical clearance was granted by Jinan City People's Hospital. All procedures followed national standards governing laboratory animal care, including the Guidelines for Ethical Review of the Welfare of Laboratory Animals (GB/T35892-2018), IGP 2012, and IAVE 2010 guidelines. Animals were acclimated for one week in controlled conditions (20–25°C; 50–70% humidity) with unrestricted food and water.

Mice were randomly assigned to four groups (n = 8 per group):

1. saline group (saline)
2. P. acnes group (P. acnes)
3. P. acnes + CHL group
4. P. acnes + SB203580 group

Acne-like lesions were induced by intradermal injection of 1×10^7 CFU of P. acnes in 50 μL BHI medium, followed immediately by daily application of 20 μL synthetic sebum. The saline group received equal volumes of saline for both procedures. Induction lasted 7 days. From days 8–21, animals in the CHL-treated group received topical application of 1.5 mL CHL twice daily for 15–20 minutes. SB203580 (5 mg/kg/day) was administered intraperitoneally on days 11, 14, and 17. The complete experimental layout appears in **Figure 2**.

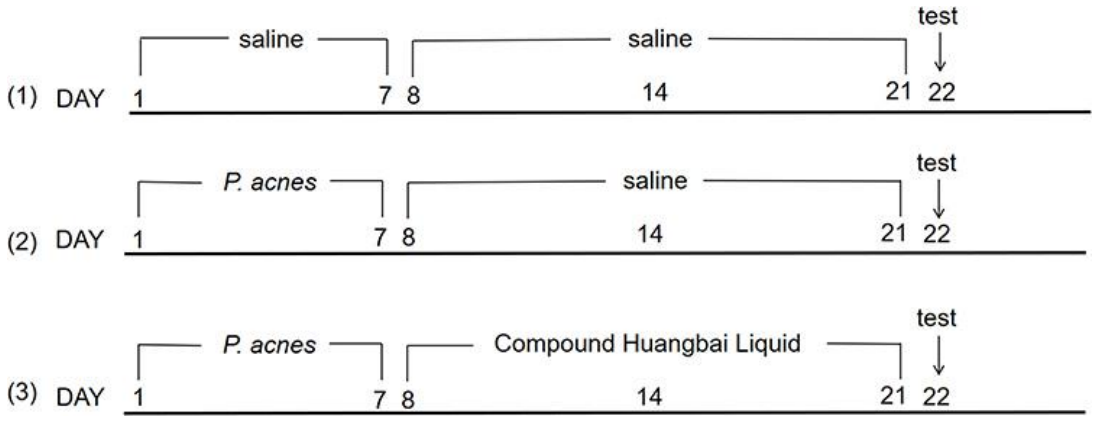

Figure 2. Experimental protocol

Histopathological and immunohistochemical analysis of skin tissue

Skin samples from all experimental groups were preserved in 4% paraformaldehyde, processed into paraffin blocks, and sectioned for hematoxylin and eosin (H&E) staining. To visualize protein expression, immunohistochemistry was conducted to assess TLR4, NF-κB p65, P38 MAPK, phospho-NF-κB p65, and phospho-p38 MAPK. The antibodies used in these assays included anti-TLR4, anti-NF-κB p65, anti-p38 MAPK, anti-phospho-NF-κB p65, and anti-phospho-p38 MAPK (all from Abcam, MA, USA). The technical procedures followed the protocol previously outlined by Chen [22]. Microscopic evaluation was used to examine pathological alterations and immunostaining patterns. Quantitative assessment was carried out using Image-Pro Plus 6.0, and protein abundance was expressed as mean optical density = integrated optical density ÷ region of interest.

Preparation of tissue homogenate

Dorsal skin tissues were excised, rinsed with chilled PBS, and blotted to remove excess moisture before weighing. Each sample was homogenized on ice using a glass homogenizer with an appropriate volume of pre-cooled PBS to yield a 10% tissue homogenate. The homogenates were centrifuged at 9400 g for 10 minutes at 4°C, and the resulting supernatants were aliquoted and stored at −80°C until subsequent assays.

Enzyme-Linked immunosorbent assay

Levels of IL-6, IL-1β, and TNF-α were quantified using ELISA kits obtained from eBioscience (San Diego, CA, USA). All measurements adhered strictly to the manufacturer's protocols. The detection limits were 3 pg/mL for IL-6, 1.2 pg/mL for IL-1β, and 3.7 pg/mL for TNF-α.

Statistical analysis

All numerical results were expressed as mean ± SEM. Statistical analyses were performed using SPSS 19.0, and graphical outputs were generated with GraphPad Prism 8.0. Differences between groups were interpreted as significant when $P < 0.05$ (*) or $P < 0.01$ (**), based on one-way ANOVA.

Results and Discussion

Compounds and target genes in Compound Huangbai Liquid

To identify the bioactive ingredients of Compound Huangbai Liquid (CHL), the herbs—Forsythiae Fructus (Lianqiao), Phellodendri chinensis Cortex (Huangbai), Honeysuckle (Jinyin Hua), Dandelion (Pugong Ying), and Centipede (Wugong)—were queried in the BATMAN-TCM platform. Compounds were selected using the criteria score ≥ 20 and $P < 0.05$. The number of retrieved constituents and their corresponding targets are summarized in **Table 1.**

A total of 165 compounds were identified across all five herbs:

- Forsythiae Fructus: 47 compounds, with 32 meeting the screening threshold
- Phellodendri chinensis Cortex: 37 compounds, 28 retained
- Honeysuckle: 72 compounds, 46 retained
- Dandelion: 8 compounds, all 8 retained
- Centipede: 7 compounds, 5 retained

(With six compounds shared among the five herbs.)

The screened compounds generated the following target gene counts:

- Forsythiae Fructus: 543 targets
- Phellodendri chinensis Cortex: 325 targets
- Honeysuckle: 853 targets
- Dandelion: 123 targets
- Centipede: 212 targets

Comprehensive details regarding individual compounds and predicted targets can be found in the Supplementary Data.

Table 1. The number of compounds and target genes in Compound Huangbai Liquid

Herbs	Total of Compounds	Number of Compounds (Cutoff ≥20, p < 0.05)	Number of Target Genes
Forsythiae Fructus (Lianqiao)	47	32	543
Phellodendri chinensis Cortex (Huangbai)	37	28	325
Honeysuckle (Jinyin Hua)	72	46	853
Dandelion (Pugong Ying)	8	8	123
Centipede (Wugong)	7	5	212

Prediction of potential targets

As summarized in **Table 2**, an initial pool of 156 acne-associated genes was collected from the GeneCards, DisGeNet, and OMIM databases. These disease-related genes were then compared with the predicted targets derived from the active constituents of Compound Huangbai Liquid, and the intersection of the two datasets was visualized using a Venn diagram **(Figure 3)**. This comparative analysis yielded 34 shared genes, representing the most plausible therapeutic targets through which Compound Huangbai Liquid may exert anti-acne effects **(Table 3)**. Among these common targets were IL1RN, TNF, UROD, SOX9, and several others.

Table 2. Acne-Related target genes

Number	Gene Symbol	Number	Gene Symbol	Number	Gene Symbol
1	VDR	53	TIMP2	105	SEMA4B
2	ACE	54	C11orf49	106	IGFBP7
3	IL17A	55	XLI	107	PEN2
4	CYP17A1	56	ATOD1	108	ARCI5
5	C1orf112	57	EEF1D	109	EZR
6	TLR4	58	NCSTN	110	DEFB4B
7	LYNX1	59	S100A7	111	CHI3L1
8	PSTPIP1	60	CD83	112	DGS
9	MEFV	61	AFND	113	LOC102723407
10	EDN1	62	PSTPIP	114	RDCCAS

11	CARD14	63	TTD1	115	FOXO1
12	LGALS7B	64	CD79A	116	GPT
13	IL36RN	65	ANGPTL3	117	PINX1
14	CYP19A1	66	PSORS11	118	RHOA
15	PPNAD4	67	CTLA4	119	CCL7
16	IGF1	68	SMIM10L2A	120	CALCA
17	MAPK14	69	CORTRD1	121	ADCY10
18	SOX9	70	S100A7A	122	HGF
19	TRAF3IP2	71	LCN2	123	ESTRR
20	DEFB4A	72	RNASE7	124	SERPINA1
21	CCL5	73	BDNF	125	HDAC9
22	IL1RAPL2	74	CDH1	126	ORI6
23	PDGFRB	75	LOC102724971	127	FTHS
24	NAP1L2	76	CAMP	128	CDK2
25	ATOD2	77	RETN	129	TNFSF12
26	UROD	78	APH1A	130	DSG3
27	IL20	79	SREBF1	131	TNFSF12-TNFSF13
28	LPL	80	NOD2	132	IL1RN
29	PLXNA2	81	PAGR1	133	LYPLAL1-DT
30	ANGPTL4	82	ACNINV3	134	PSORS4
31	NLRP3	83	PAPAS	135	ABCD2
32	LEP	84	XLP2	136	CD2BP1
33	LGALS7	85	PSORS1	137	DCD
34	LYZ	86	FOXO3	138	ADIPOQ
35	FGFR2	87	DSG1	139	PPARD
36	SUGCT	88	CGD5	140	MMP2
37	SFPQ	89	PSORS14	141	NOS2
38	HSD3B1	90	PCNX3	142	TNF
39	ABOLM	91	PSEN1	143	EGF
40	RBP4	92	TLR2	144	IL1A
41	STGD1	93	WNT10A	145	AKT1
42	DEFB1	94	GALNS	146	IL10
43	CRH	95	SETBP1	147	PTGS2
44	NOS1	96	SMIM10L2B	148	EGFR
45	HSD17B3	97	UBE2E1	149	IL1B
46	IL22	98	HDAC8	150	SOD1
47	DNMT1	99	GAST	151	AR
48	SRXY1	100	CANDF1	152	PPARG
49	BCYM4	101	TNFRSF1B	153	IL6
50	PSENEN	102	AD3	154	CXCL8
51	ADORA2A-AS1	103	IGHA1	155	MMP9
52	APOC3	104	MCOPCB10	156	THBD

Table 3. Potential targets of acne treatment

Number	Gene Symbol	Number	Gene Symbol	Number	Gene Symbol
1	IL1RN	13	ACE	25	THBD
2	TNF	14	VDR	26	NOS1
3	UROD	15	BDNF	27	IL10
4	SOX9	16	IGF1	28	SREBF1
5	AR	17	IL6	29	EDN1
6	EZR	18	FGFR2	30	IL1B
7	CALCA	19	CXCL8	31	CRH
8	CYP19A1	20	GPT	32	PPARG

9	TLR4	21	HDAC9	33	SUGCT
10	PPARD	22	CYP17A1	34	LEP
11	NOD2	23	CCL5		
12	PTGS2	24	NOS2		

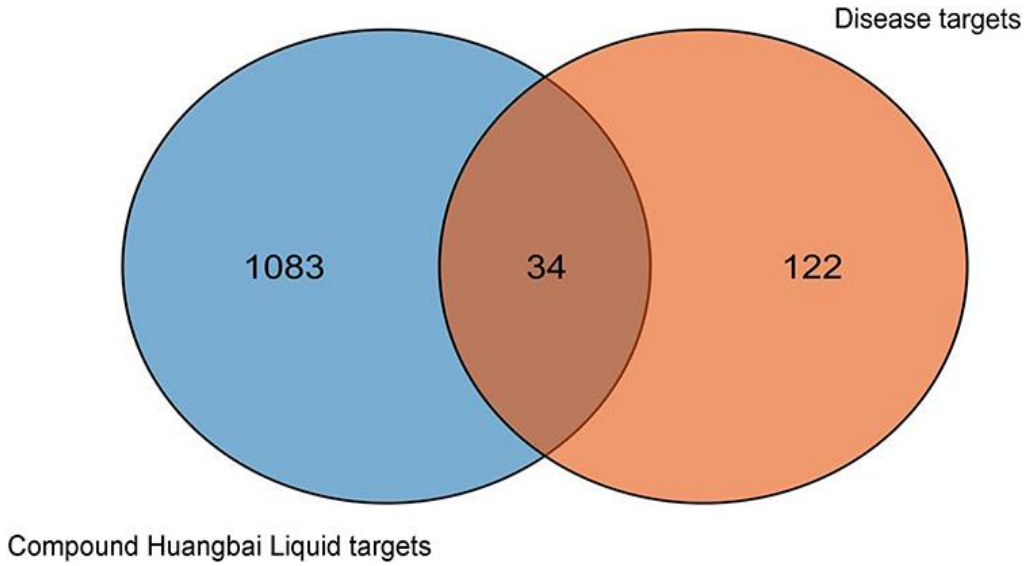

Figure 3. Venn diagram illustrating the overlap between potential targets of Compound Huangbai Liquid and genes associated with acne.

Protein–Protein Interaction (PPI) network construction

The 34 potential targets were submitted to the STRING database to generate a protein–protein interaction dataset, which was then imported into Cytoscape 3.9.1 for visualization and refinement. The resulting PPI network is displayed in **Figures 4a and 4b**, comprising 31 nodes and 221 edges, with an average node degree of 14.258. In the network, proteins represented by larger circles and deeper red hues indicate higher centrality, identifying them as key nodes, including IL-6, TNF, and IL-1B, which play core roles in the interaction network.

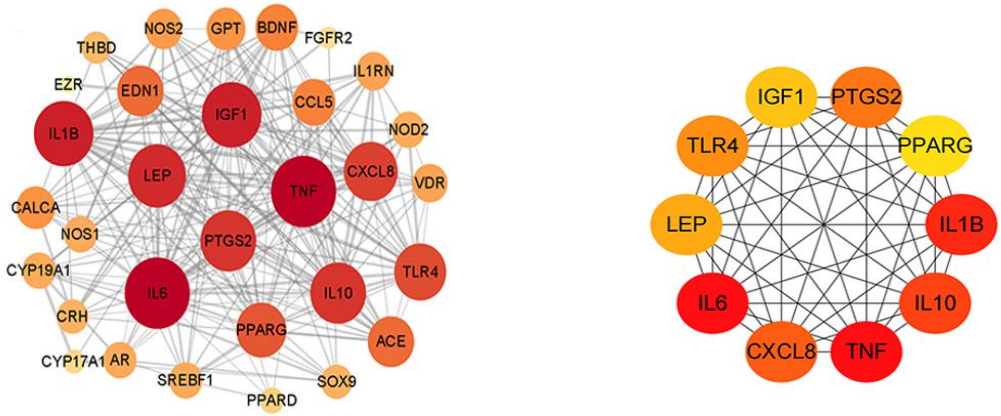

a) b)

Figure 4. PPI network of targets associated with Compound Huangbai Liquid in acne treatment. (a) Complete PPI network of the 34 potential therapeutic targets. (b) PPI network showing the top 10 targets ranked by degree. Node colors ranging from red to orange indicate decreasing degree values.

GO and pathway analysis

The 34 overlapping targets were subjected to enrichment analysis using bioinformatics.com.cn. The top 20 terms in biological process (BP), cellular component (CC), and molecular function (MF) with $P < 0.05$ were selected and are shown in **Figure 5a.**

- BP enrichment indicated involvement in cellular response to lipid, response to lipopolysaccharide, regulation of secretion, hormone response, and multicellular organism processes.
- CC enrichment highlighted components such as the basal part of the cell, receptor complexes, rafts and membrane sides, and transport vesicles.
- MF enrichment included receptor ligand activity, nuclear receptor activity, hormone activity, heme binding, and G protein-coupled receptor binding.

These results suggest that the anti-acne effects of CHL likely arise from coordinated actions across multiple biological processes, reflecting a complex and synergistic mechanism.

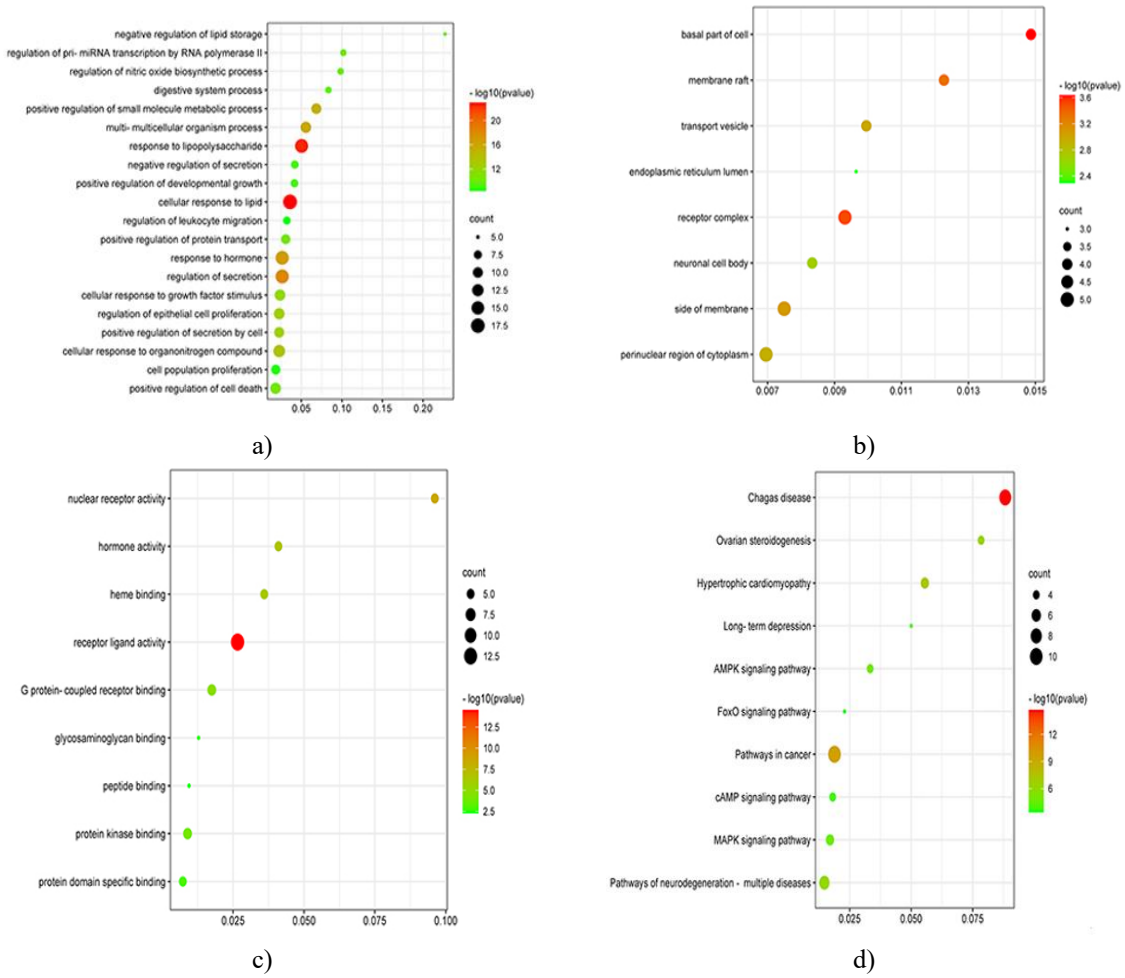

Figure 5. GO and KEGG pathway enrichment analysis. (a) Biological process (BP) categories; (b) Cellular component (CC) categories; (c) Molecular function (MF) categories; (d) KEGG pathway analysis.

In the KEGG pathway analysis, the 34 identified targets were mapped to 10 significant pathways ($P < 0.05$), including Chagas disease and cancer-related pathways. In the bubble diagram **(Figure 5d)**, larger bubbles indicate pathways enriched with more genes, and darker red colors correspond to higher statistical significance (smaller P values).

To explore the complex interactions between herbs, compounds, targets, and disease, Cytoscape 3.9.1 was used to generate the TCM-compound-target-disease network and the disease-target-pathway network **(Figures 6a and 6b)**. The TCM-compound-target-disease network contained 106 nodes (1 disease, 5 herbs, 68 compounds, 32 targets) connected by 308 edges. Analysis of node degree **(Table 2)** revealed that the top five compounds—3-Methyl-2-(2-Pentenyl)-2-Cyclopenten-1-One, beta-Pinene, carvacrol, ursolic acid, and D-Limonene—interacted with 13, 12, 9, 7, and 7 targets, respectively. On the target side, the most connected nodes were AR, VDR, PPARD, PTGS2, and IL1B, which were associated with 35, 20, 15, 14, and 13 compounds, respectively, indicating their potential central role in CHL's anti-acne effects.

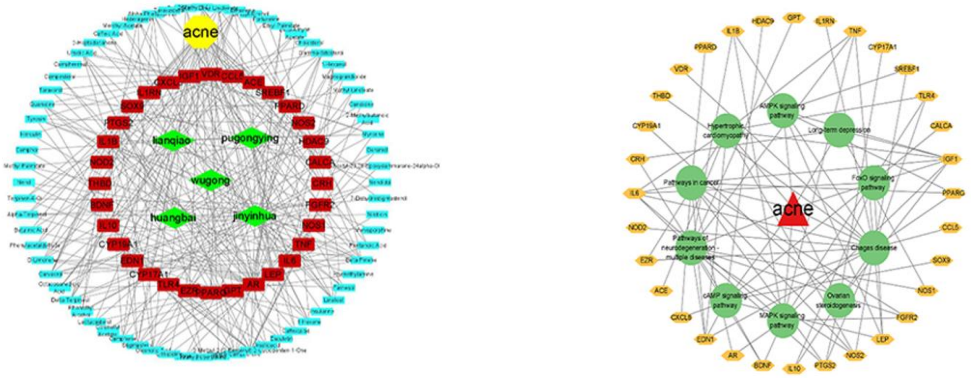

a) b)

Figure 6. Network construction. (a) TCM-compound-target-disease network showing the relationships between Compound Huangbai Liquid and acne. The green nodes represent the five herbs in CHL, blue diamonds denote major active compounds, red nodes indicate core targets, and the yellow node represents acne. (b) Disease-target-pathway network of core targets, where orange nodes indicate core targets, the red triangle represents acne, and green circles correspond to the top 10 GO annotation results.

Using the top 10 KEGG pathways and identified targets, a disease-target-pathway network was generated in Cytoscape 3.9.1. The resulting network **(Figure 6b)** included 43 nodes connected by 86 edges. Among the pathways, Chagas disease had the highest gene enrichment with 19 genes, followed by pathways in cancer (10 genes) and Hypertrophic cardiomyopathy (8 genes). The detailed KEGG map for Chagas disease is shown in **Figure 7.**

Integrating results from PPI analysis, GO-BP enrichment, KEGG pathway analysis, and the disease-target-pathway network, we identified six key molecular targets through which CHL may modulate acne-related pathology: TLR4, NF-κB, p38 MAPK, TNFα, IL-6, and IL-1β.

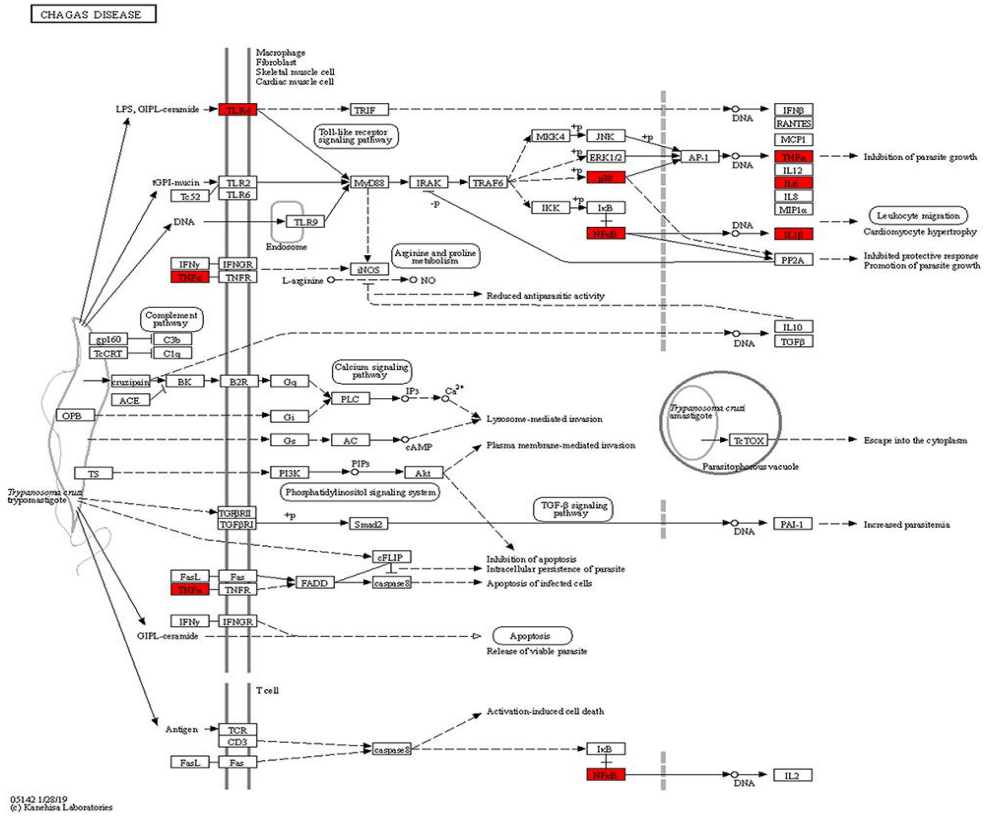

Figure 7. Anti-acne pathways of Compound Huangbai Liquid (CHL), with red squares indicating the core therapeutic targets within the pathways.

Compound Huangbai Liquid attenuated acne-like skin lesions induced by P. acnes

The condition of the mice's back skin on day 22 is shown in **Figure 8a**. The saline group displayed normal, healthy skin. In contrast, the P. acnes group showed marked redness, swelling, raised papules, and areas of hemorrhage. Following treatment with CHL, most of the elevated papules had nearly disappeared. A similar improvement was observed in the SB203580-treated group, where papules were markedly reduced and the skin exhibited scabbing.

Histopathological examination using H&E staining further illustrated the skin changes **(Figure 8b)**. The P. acnes group developed acne-like lesions that were absent in the saline group. As shown in **Figure 8b**, the sebaceous glands in the epidermis and subcutaneous hair follicles were intact in the saline group. In the P. acnes group, there was epidermal thickening, prominent thickening of the granular and spinous layers of hair follicle epithelium, and excessive keratinization. Large accumulations of keratinized material were observed at the follicular openings and infundibular regions, which were dilated. Additionally, dermal hair follicles were increased in number, and adjacent follicles tended to fuse.

Treatment with CHL reduced hair follicle dilation, epidermal thickening, and the number of hair follicles, while keratinization became more diffuse and relaxed. The therapeutic effects of SB203580 were comparable to CHL. Quantitative assessment using disease scores **(Figure 8c)** and pathology scores **(Figure 8d)**, based on previously established criteria [23], confirmed that CHL significantly alleviated acne-like skin lesions in mice.

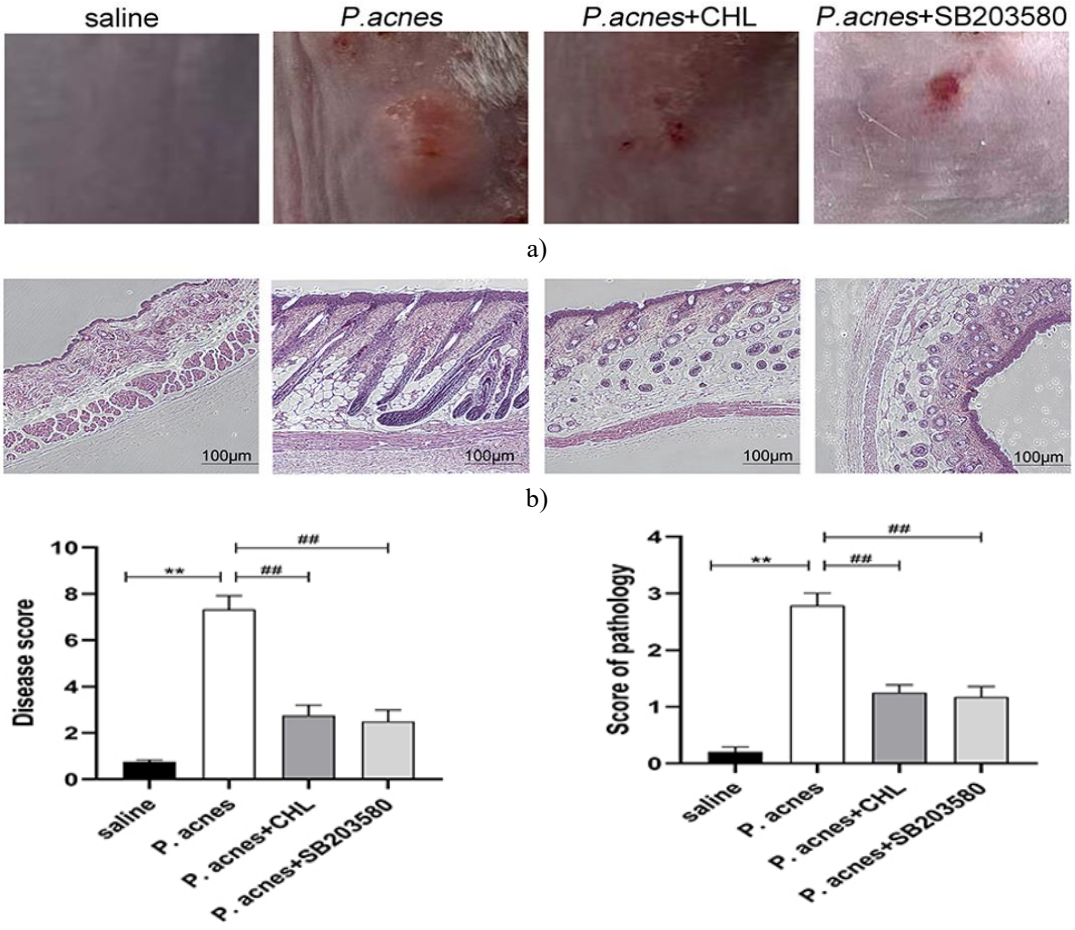

Figure 8. Effects of Compound Huangbai Liquid on P. acnes-induced acne-like skin lesions. (a) Representative images of back skin after 21 days for the saline group, P. acnes group, CHL-treated group, and SB203580-treated group. (b) Histological evaluation of skin sections using hematoxylin and eosin (H&E) staining at 10× magnification. (c) Quantification of disease severity scores. (d) Quantification of pathology scores. Data are presented as mean ± SEM. *$p < 0.05$ and **$p < 0.01$ indicate significant differences versus the saline group; #$p < 0.05$ and ##$p < 0.01$ indicate significant differences versus the P. acnes group ($n = 6$).

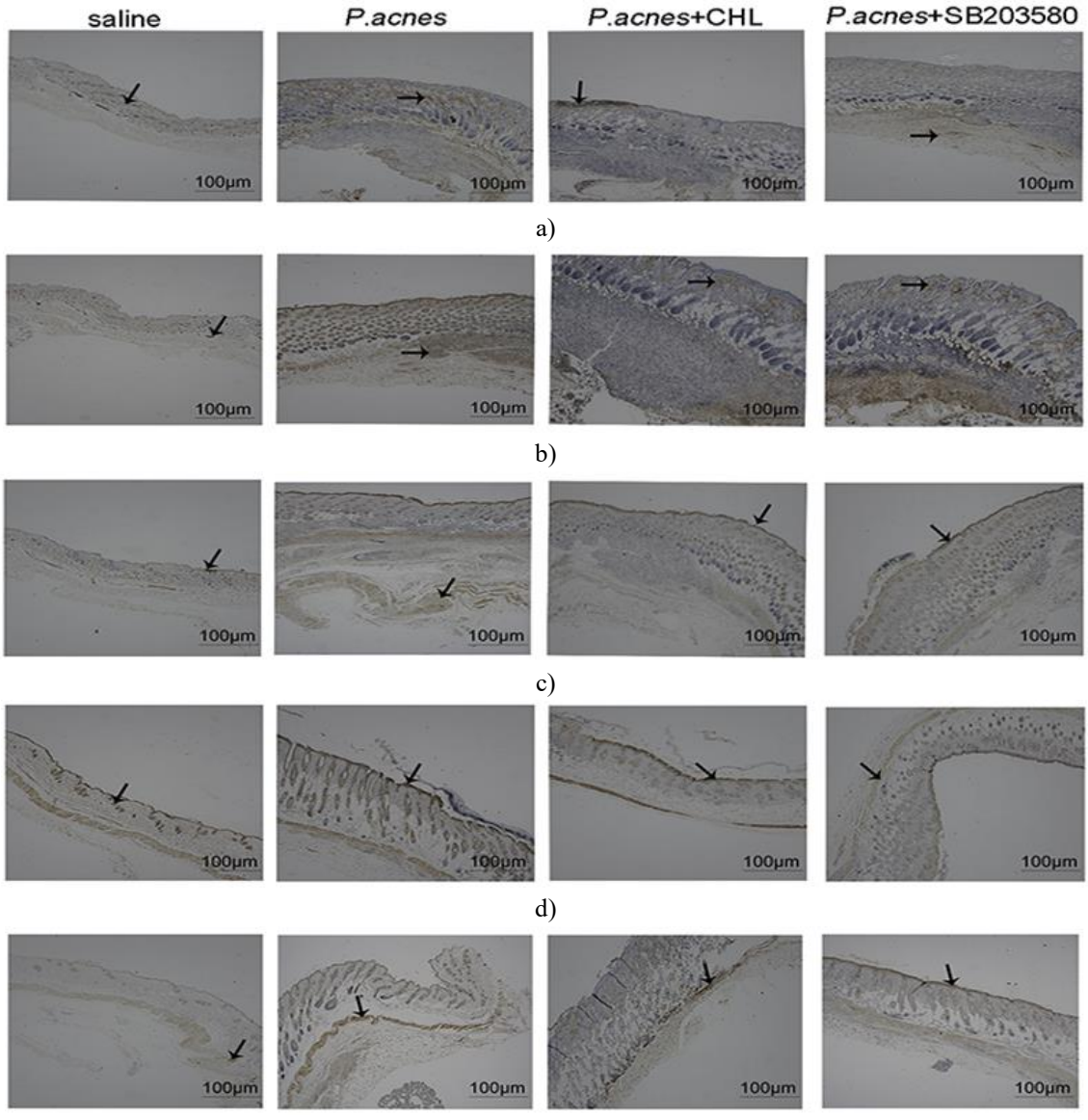
saline
P.acnes
P.acnes+CHL
P.acnes+SB203580
100μm
a)
b)
c)
d)
e)

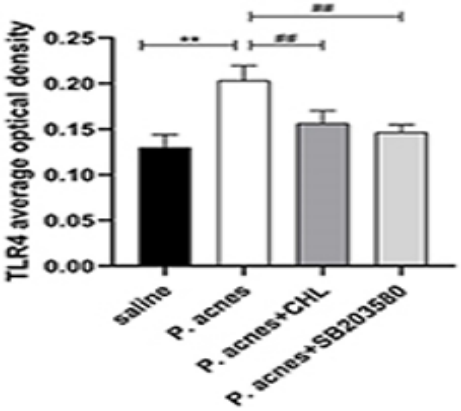
TLR4 average optical density
0.25
0.20
0.15
0.10
0.05
0.00
**
##
##
saline
P. acnes
P. acnes+CHL
P. acnes+SB203580

f)

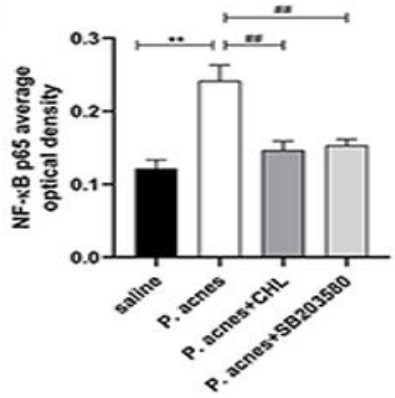
NF-κB p65 average optical density
0.3
0.2
0.1
0.0
**
##
##
saline
P. acnes
P. acnes+CHL
P. acnes+SB203580

g)

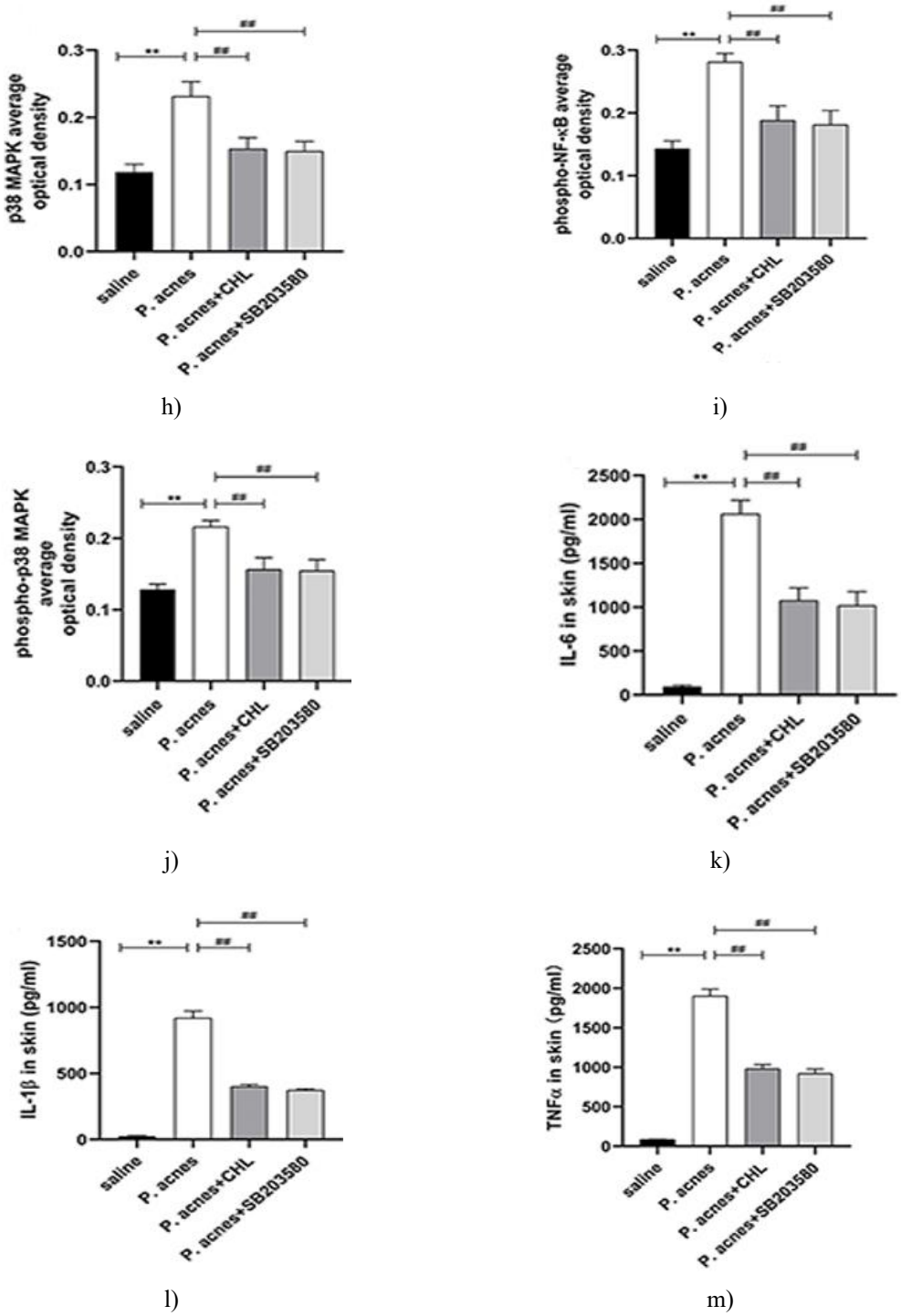

Figure 9. Effects of Compound Huangbai Liquid (CHL) on TLR4/NF-κB/p38 MAPK signaling and cytokine expression. (a–e) Immunohistochemical staining of TLR4, NF-κB p65, p38 MAPK, phospho-NF-κB p65, and phospho-p38 MAPK in mouse skin. (F–J) Quantification of protein expression levels. (K–M) ELISA detection of IL-6, IL-1β, and TNFα in skin tissues. Data are expressed as mean ± SEM. *p < 0.05, *p < 0.01 vs. saline group; #p < 0.05, ##p < 0.01 vs. P. acnes group (n = 6). Pictures at 10× magnification.

CHL suppresses TLR4/NF-κB/p38 MAPK signaling and cytokine production

To verify whether CHL alleviates acne through TLR4, NF-κB, and p38 MAPK pathways, mice were treated with CHL and skin tissues analyzed. Immunohistochemistry showed that P. acnes induced significant upregulation of TLR4 **(Figure 9f)**, NF-κB p65 **(Figure 9g)**, p38 MAPK **(Figure 9h)**, phospho-NF-κB p65 **(Figure 9i)**, and phospho-p38 MAPK **(Figure 9j)** compared with the saline group ($p < 0.01$). Treatment with CHL or SB203580 significantly reduced the expression of these proteins ($p < 0.05$ or 0.01) relative to P. acnes alone.

ELISA results demonstrated that IL-6 **(Figure 9k)**, IL-1β **(Figure 9l)**, and TNFα **(Figure 9m)** levels were significantly elevated in the P. acnes group ($p < 0.01$ vs. saline), and administration of CHL or SB203580 substantially decreased their expression ($p < 0.01$ vs. P. acnes).

Acne is a chronic inflammatory skin disorder influenced by hyperseborrhea, abnormal keratinization, Cutibacterium acnes, and inflammation [13]. In China, both clinicians and patients increasingly prefer Compound Huangbai Liquid (CHL), a natural and relatively safe treatment option. Historically, TCM lacked molecular-level mechanistic evidence and was not widely accepted [24, 25]. The emergence of network pharmacology in 2007–2008 [26, 27] allows the identification of active compounds, target genes, and molecular mechanisms, providing a scientific rationale for TCM therapies.

Through the BATMAN-TCM database, 165 active ingredients of CHL were identified. The primary anti-inflammatory compounds included 3-Methyl-2-(2-Pentenyl)-2-Cyclopenten-1-One, beta-Pinene, carvacrol, ursolic acid, and D-Limonene. For instance, 3-Methyl-2-(2-Pentenyl)-2-Cyclopenten-1-One reduces Vitamin D receptor (VDR) expression and suppresses sebaceous gland hyperactivity [28]. Ursolic acid inhibits TNFα expression and reduces IL-1β and IL-6 secretion in vitro [29], illustrating that CHL acts synergistically on multiple targets.

Immunohistochemistry and ELISA demonstrated that P. acnes significantly increased TLR4, NF-κB, p38 MAPK, IL-6, IL-1β, and TNFα levels, consistent with prior findings that TLR4 activation in keratinocytes triggers NF-κB and MAPK signaling, resulting in cytokine production [12, 30, 31]. IL-1β contributes to pilosebaceous unit pathology, keratinocyte proliferation, and microcomedone formation, and is upregulated around hair follicles in inflammatory acne [32–34]. IL-6, induced by IL-1β, amplifies the inflammatory response [31, 34], and TNFα regulates sebaceous lipogenesis and lipid droplet formation [35–37].

In the P. acnes + CHL group, expression of TLR4, NF-κB, p38 MAPK, IL-6, IL-1β, and TNFα was significantly reduced. Network analysis highlighted TLR4, IL-6, IL-1β, and TNFα as CHL targets, while KEGG analysis implicated the Chagas disease signaling pathway, which involves NF-κB and p38 MAPK. Collectively, these results suggest that CHL exerts anti-inflammatory effects by suppressing TLR4/NF-κB/p38 MAPK activation and decreasing IL-6, IL-1β, and TNFα secretion [29].

Conclusion

In conclusion, network pharmacology combined with experimental validation shows that CHL treats acne through multi-component, multi-target, and multi-pathway mechanisms, particularly by modulating TLR4/NF-κB/p38 MAPK signaling and associated cytokines, providing a mechanistic foundation for its clinical application in acne.

Acknowledgments: None

Conflict of Interest: None

Financial Support: None

Ethics Statement: None

References

1. Harper JC, Thiboutot DM. Pathogenesis of acne: recent research advances. Adv Dermatol. 2003;19:1–10.
2. Tanghetti EA. The role of inflammation in the pathology of acne. J Clin Aesthet Dermatol. 2013;6(9):27.
3. Williams HC, Dellavalle RP, Garner S. Acne vulgaris. Lancet. 2012;379(9813):361–72. doi:10.1016/S0140-6736(11)60321-8
4. Li X, He C, Chen Z, Zhou C, Gan Y, Jia Y. A review of the role of sebum in the mechanism of acne pathogenesis. J Cosmet Dermatol. 2017;16(2):168–73. doi:10.1111/jocd.12345
5. Tan JK, Gold LS, Alexis AF, Harper JC. Current concepts in acne pathogenesis: pathways to inflammation. Semin Cutan Med Surg. 2018;37:60–2.
6. Ingham E, Eady EA, Goodwin CE, Cove JH, Cunliffe WJ. Pro-inflammatory levels of interleukin-1î±-like bioactivity are present in the majority of open comedones in acne vulgaris. J Investig Dermatol. 1992;98(6):895–901. doi:10.1111/1523-1747.ep12460324

7. Li ZJ, Choi DK, Sohn KC, Seo MS, Lee HE, Lee Y, et al. Propionibacterium acnes activates the NLRP3 inflammasome in human sebocytes. J Invest Dermatol. 2014;134(11):2747-56. doi:10.1038/jid.2014.221. Epub 2014 May 12. PMID: 24820890.
8. Kistowska M, Gehrke S, Jankovic D, Kerl K, Fettelschoss A, Feldmeyer L, et al. IL-1β drives inflammatory responses to propionibacterium acnes in vitro and in vivo. J Invest Dermatol. 2014;134(3):677-85. doi:10.1038/jid.2013.438. Epub 2013 Oct 24. PMID: 24157462.
9. Mastrofrancesco A, Kokot A, Eberle A, Gibbons NC, Schallreuter KU, Strozyk E, et al. KdPT, a tripeptide derivative of alpha-melanocyte-stimulating hormone, suppresses IL-1 beta-mediated cytokine expression and signaling in human sebocytes. J Immunol. 2010;185(3):1903-11. doi:10.4049/jimmunol.0902298. Epub 2010 Jul 7. PMID: 20610647.
10. Wang D, Duncan B, Li X, Shi J. The role of NLRP3 inflammasome in infection-related, immune-mediated and autoimmune skin diseases. J Dermatol Sci. 2020;98(3):146–51. doi:10.1016/j.jdermsci.2020.03.001
11. Dreno B, Gollnick HP, Kang S, Thiboutot D, Bettoli V, Torres V, et al. Understanding innate immunity and inflammation in acne: implications for management. J Eur Acad Dermatol Venereol. 2015 Jun;29 Suppl 4:3-11. doi:10.1111/jdv.13190. PMID: 26059728.
12. Lee YB, Byun EJ, Kim HS. Potential role of the microbiome in acne: a comprehensive review. J Clin Med. 2019;8(7):987. doi:10.3390/jcm8070987
13. Cong T-X, Hao D, Wen X, Li X-H, He G, Jiang X. From pathogenesis of acne vulgaris to anti-acne agents. Arch Dermatol Res. 2019;311(5):337–49. doi:10.1007/s00403-019-01908-x
14. Wu P, Liang S, He Y, Lv R, Yang B, Wang M, et al. Network pharmacology analysis to explore mechanism of Three Flower Tea against nonalcoholic fatty liver disease with experimental support using high-fat diet-induced rats. Chin Herb Med. 2022;14(2):273-82. doi:10.1016/j.chmed.2022.03.002. PMID: 36117665; PMCID: PMC9476824.
15. Chen H-Y, Lin Y-H, Chen Y-C. Identifying Chinese herbal medicine network for treating acne: implications from a nationwide database. J Ethnopharmacol. 2016;179:1–8. doi:10.1016/j.jep.2015.12.032
16. Chiang CC, Cheng WJ, Lin CY, Lai KH, Ju SC, Lee C, et al. Kan-Lu-Hsiao-Tu-Tan, a traditional Chinese medicine formula, inhibits human neutrophil activation and ameliorates imiquimod-induced psoriasis-like skin inflammation. J Ethnopharmacol. 2020;246:112246. doi:10.1016/j.jep.2019.112246. Epub 2019 Sep 17. PMID: 31539577.
17. Ghafourian A, Ghafourian S, Sadeghifard N, Mohebi R, Shokoohini Y, Nezamoleslami S, et al. Vitiligo: symptoms, pathogenesis and treatment. Int J Immunopathol Pharmacol. 2014;27(4):485-9. doi:10.1177/039463201402700403. PMID: 25572727.
18. Uzun S, Wang Z, McKnight TA, Ehrlich P, Thanik E, Nowak-Wegrzyn A, et al. Improvement of skin lesions in corticosteroid withdrawal-associated severe eczema by multicomponent traditional Chinese medicine therapy. Allergy Asthma Clin Immunol. 2021;17(1):68. doi:10.1186/s13223-021-00555-0. PMID: 34243796; PMCID: PMC8268267.
19. Bedout VD, Nichols AJ. Traditional Chinese medicine approaches. In: Integrative Dermatology. Springer; 2021:235–48.
20. Shao L, Zhang B. Traditional Chinese medicine network pharmacology: theory, methodology and application. Chin J Nat Med. 2013;11(2):110–20. doi:10.1016/S1875-5364(13)60037-0
21. Li H, Zhao L, Zhang B, Jiang Y, Wang X, Guo Y, et al. A network pharmacology approach to determine active compounds and action mechanisms of ge-gen-qin-lian decoction for treatment of type 2 diabetes. Evid Based Complement Alternat Med. 2014;2014:495840. doi:10.1155/2014/495840. Epub 2014 Jan 16. PMID: 24527048; PMCID: PMC3914348.
22. Chen W, He L, Zhong L, Sun J, Zhang L, Wei D, et al. Identification of active compounds and mechanism of huangtu decoction for the treatment of ulcerative colitis by network pharmacology combined with experimental verification. Drug Des Devel Ther. 2021;15:4125-40. doi:10.2147/DDDT.S328333. PMID: 34616145; PMCID: PMC8487861.
23. Kolar SL, Tsai C-M, Torres J, Fan X, Li H, Liu GY. Propionibacterium acnes–induced immunopathology correlates with health and disease association. JCI Insight. 2019;4(5). doi:10.1172/jci.insight.124687
24. Qiu J. Traditional medicine: a culture in the balance. Nature. 2007;448(7150):126–9. doi:10.1038/448126a
25. Stone R. Lifting the veil on traditional Chinese medicine. Am Assoc Adv Sci. 2008;2008:709–10.
26. Hopkins AL. Network pharmacology. Nat Biotechnol. 2007;25(10):1110–1. doi:10.1038/nbt1007-1110

27. Hopkins AL. Network pharmacology: the next paradigm in drug discovery. Nat Chem Biol. 2008;4(11):682–90. doi:10.1038/nchembio.118
28. Makrantonaki E, Ganceviciene R, Zouboulis CC. An update on the role of the sebaceous gland in the pathogenesis of acne. Dermato-Endocrinology. 2011;3(1):41–9. doi:10.4161/derm.3.1.13900
29. Soleymani S, Farzaei MH, Zargaran A, Niknam S, Rahimi R. Promising plant-derived secondary metabolites for treatment of acne vulgaris: a mechanistic review. Arch Dermatol Res. 2020;312(1):5–23. doi:10.1007/s00403-019-01968-z
30. Jugeau S, Tenaud I, Knol AC, Jarrousse V, Quereux G, Khammari A, et al. Induction of toll-like receptors by Propionibacterium acnes. Br J Dermatol. 2005;153(6):1105-13. doi:10.1111/j.1365-2133.2005.06933.x. PMID: 16307644.
31. Chen Y, Ji N, Pan S, Zhang Z, Wang R, Qiu Y, et al. Roburic Acid Suppresses NO and IL-6 Production via Targeting NF-κB and MAPK Pathway in RAW264.7 Cells. Inflammation. 2017;40(6):1959-66. doi:10.1007/s10753-017-0636-z. PMID: 28761990.
32. Guy R, Green MR, Kealey T. Modeling acne in vitro. J Investig Dermatol. 1996;106(1):176–82. doi:10.1111/1523-1747.ep12329907
33. Ständer S, Schmelz M, Metze D, Luger T, Rukwied R. Distribution of cannabinoid receptor 1 (CB1) and 2 (CB2) on sensory nerve fibers and adnexal structures in human skin. J Dermatol Sci. 2005;38(3):177–88. doi:10.1016/j.jdermsci.2005.01.007
34. Liu X, Ye F, Xiong H, Hu DN, Limb GA, Xie T, et al. IL-1β induces IL-6 production in retinal Müller cells predominantly through the activation of p38 MAPK/NF-κB signaling pathway. Exp Cell Res. 2015;331(1):223-31. doi:10.1016/j.yexcr.2014.08.040. Epub 2014 Sep 17. PMID: 25239226.
35. Sethi G, Sung B, Aggarwal BB. TNF: a master switch for inflammation to cancer. Front Biosci. 2008;13(2):5094–107. doi:10.2741/3066
36. Choi JJ, Park MY, Lee HJ, Yoon DY, Lim Y, Hyun JW, et al. TNF-α increases lipogenesis via JNK and PI3K/Akt pathways in SZ95 human sebocytes. J Dermatol Sci. 2012;65(3):179-88. doi:10.1016/j.jdermsci.2011.11.005. Epub 2011 Nov 20. PMID: 22305016.
37. Rico MJ. The role of inflammation in acne vulgaris. Pract Dermatol. 2013;8:22–33.